Pergamon

0277-5387(95)00023-2

Polyhedron Vol. 14, No. 15-16, pp. 2071-2077, 1995
Copyright © 1995 Elsevier Science Ltd
Printed in Great Britain. All rights reserved
0277-5387/95 $9.50+0.00

COORDINATION REACTION OF IRON(III) WITH 8-HYDROXY-7-[(2-HYDROXY-5-CARBOXYPHENYL)AZO]-5-QUINOLINESULPHONIC ACID: EVIDENCE FOR KINETIC LINKAGE ISOMERISM

ZHI-PING BAI, JINSAI HIDAKA

Department of Chemistry, University of Tsukuba, Tsukuba, Ibaraki 305, Japan

and

HISAHIKO EINAGA*

Department of Applied Chemistry, Faculty of Engineering, Nagoya Institute of Technology, Gokiso-cho, Showa-ku, Nagoya 466, Japan

(*Received* 27 *September* 1994; *accepted* 21 *December* 1994)

Abstract—Coordination reaction kinetics of a bifunctional multidentate ligand, 8-hydroxy-7-[(2-hydroxy-5-carboxyphenyl)-azo]-5-quinolinesulphonic acid (H_4hcqs), to iron(III) has been investigated in an aqueous 0.10 mol dm^{-3} sodium perchlorate solution at 22°C. This ligand initially coordinates to the metal ion to form an intermediate complex with its bidentate quinolinolato(*N-O*) moiety, $Fe(H_2hcqs\text{-}N,O)^+$, which then transforms to a complex with its terdentate dihydroxyazo(*O-N-O*) moiety, $Fe(H_2hcqs\text{-}O,N,O)^+$, with the stability constant (β_{11}) of log β_{11} (mol^{-1} dm^3) of 18.32 ± 0.11, thus showing a kinetic linkage isomerism. The first step proceeds through the parallel pathways of $Fe^{3+} + H_2hcqs^{2-}$ (k_{32}) and $FeOH^{2+} + H_4hcqs$ (k_{20}) with the composite rate constant of $k_{32} + k_{20}K_{a(qyNH)}$, K_{OH} (mol^{-1} dm^3 s^{-1}) of $1.92 \pm 0.35 \times 10^3$ showing the greater importance of the pathway of k_{20} as compared with that of k_{32}, where $K_{a(qyNH)}$ and K_{OH} are the protonation constant of the quinolinol nitrogen of H_4hcqs and the hydrolysis constant of Fe^{3+}, respectively; the second step of the linkage isomerization from $Fe(H_2hcqs\text{-}N,O)^+$ to $Fe(H_2hcqs\text{-}O,N,O)^+$ has the rate constant (k_{isom}) of $1.3 \pm 0.1 \times 10^{-1}$ s^{-1}. Thermodynamic and kinetic characteristics of these sequential reactions and those for the related ligands to the metal ion are described in detail.

The behaviour of coordination and dissociation of metal ions in a ligating environment having many donating sites is an interesting topic in bioinorganic chemistry and is of recent concern. Previously, we synthesized a new bifunctional multidentate ligand, 8-hydroxy-7-[(2-hydroxy-5-carboxyphenyl)-azo]-5-quinolinesulphonic acid (**1**, H_4hcqs), capable of taking either bidentate quinolinolato(*N-O*) coordination or terdentate dihydroxyazo(*O-N-O*) coordination, owing to steric restrictions among its ligating groups on the quinoline ring. In our earlier papers,[1,2] it was reported that **1** selectively coordinates to iron(II) with the bidentate moiety but

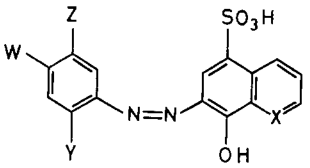

	X =	Y =	Z =	W =
1 (H_4hcqs)	N	OH	COOH	H
2 (H_4hcns)	CH	OH	COOH	H
3 (H_3cqs)	N	H	H	COOH

---

* Author to whom correspondence should be addressed.

it exhibits a linkage isomerism in its reaction to aluminium(III) between the bidentate and the terdentate coordination modes, the former being less stable and slowly transforming to the latter. Here, a new concern arises how **1** coordinates to iron(III), because this metal ion usually takes a high-spin d^5-electronic configuration in the complexes with *O* and/or *N* donor atoms.

This paper concerns the coordination reaction characteristics of **1** to iron(III) in comparison with those of three reference ligands, i.e. 4-hydroxy-3-[(2 - hydroxy - 5 - carboxyphenyl)azo] - 1 - naphthalenesulphonic acid (**2**, H_4hcns) capable of taking the terdentate dihydroxyazo coordination mode and 7-[(4-carboxyphenyl)azo]-8-hydroxy-5-quionolinesulphonic (**3**, H_3cqs) and 8-hydroxy-5-quinolinesulphonic (**4**, H_2hqs) acids taking the bidentate quinolinolato coordination mode.

EXPERIMENTAL

Materials

The syntheses of the ligands **1**–**3** have been described in a previous paper.[2] The ligand **4** was supplied by the Aldrich Chemical Co., Ltd. An aqueous solution of iron(III) was prepared as has been described elsewhere.[3]

Measurements

The apparatus and the general procedures have been presented in previous papers.[1,2] The equilibrium and kinetics were investigated in an aqueous 0.10 mol dm^{-3} $NaClO_4$ solution at 22.0±0.1°C. The formation of iron(III) complex was monitored spectrophotometrically at 502 nm for that with **1**, 540 nm for that with **2**, 497 nm for that with **3** and 605 nm for that with **4**.

RESULTS AND DISCUSSION

Coordination mode of the complex

Electronic absorption spectra of **1** and its iron(III) complex as well as those of the related ligands and their iron(III) complexes are depicted in Fig. 1.

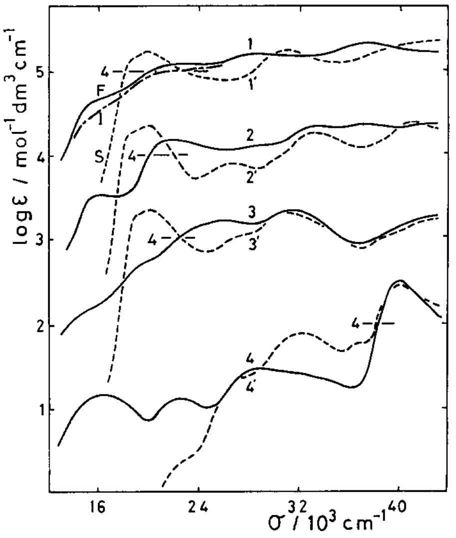

Fig. 1. Absorption spectra of the ligands and their iron(III) complexes. 1 (=F): Fe(H_2hcqs-*O*,*N*,*O*)$^+$ (pH 2.30) ; 2 : Fe(Hhcns) (pH 2.30) ; 3 : Fe(Hcqs)$^+$ (pH 2.30) ; 4 : Fe(hqs)$^+$ (pH 2.30) ; 1′(=S) : H_4hcqs (pH 2.30) ; 2′ : H_3hcns$^-$; 3′ : H_3cqs (pH 2.30), 4′: H_2hqs (pH 2.30) and I : The spectrum corresponding to that of the intermediate complex of Fe(H_2hcqs-*N*,*O*)$^+$, which was recorded 4 s after the mixing of iron(III) and **1**; 0.10 mol dm^{-3} ($NaClO_4$), 22°C.

The iron(III) complexes of **2** and **3** showed no spectral shift with time, whereas the iron(III) complex of **1** showed a slow spectral shift in the early stage of the formation reaction subsequent to a rapid spectral change from **1** to an intermediate complex. The spectrum of this intermediate complex recorded by a time-resolved mode after 4 s is also depicted in Fig. 1 (Spectrum I). It is evident from Fig. 1 that the Spectrum I of the iron(III)–**1** system has the same absorption maxima as the spectrum of the iron(III)–**3** one in the spectral region below 25 × 10^3 cm^{-1}, to which a $\pi^* \leftarrow \pi$ transition of the azo chromophore coupled with aromatic and heterocyclic chromophores and a charge-transfer transition from this azo chromophore to iron(III) contribute, i.e. 15.4 × 10^3, *ca* 20 × 10^3 and 24.0 × 10^3 cm^{-1} for the iron(III)–**1** system (Spectrum I) and 15.3 × 10^3 (shoulder), *ca* 20 × 10^3 and 23.5 × 10^3 cm^{-1} for the iron(III)–**3** one, and that the final spectrum of the complex (Spectrum F) has the same absorption maxima as the spectrum of the iron(III)–**2** one, i.e. 15.3 × 10^3 (shoulder) and 22.0 × 10^3 cm^{-1} for the iron(III)–**1** one (Spectrum F) and 16.0 × 10^3 and 22.0 × 10^3 cm^{-1} for the iron(III)–**2** one. These results indicate that the complex formation reaction of iron(III) with **1** proceeds via the *N-O* coordination mode as an intermediate to the final *O-N-O* coordination mode, thus showing a kinetic linkage isomerism.

Incidentally, it is noted from the spectral characteristics of the ligands **1**–**4** and their iron(III) complexes that the absorption bands of the lowest energy around the 16 × 10^3 cm^{-1} region can be assigned to a ligand-to-metal charge-transfer transition including the azo chromophore of the ligands on the basis of d^5-electronic structure of the central metal atom.

Formation and stability

A preliminary study revealed the formation of the iron(III) complex of **1** in an acidic aqueous solution of pH 1–3 at room temperature. Hence, the formation equilibrium of the iron(III) complex with the *O-N-O* coordination mode, $\mathrm{Fe(H_2hcqs\text{-}}O,N,O)_n^{(3-2n)+}$, can be expressed as follows,[2]

$$\mathrm{Fe^{3+}} + n\mathrm{H_4hcqs} \rightleftharpoons \mathrm{Fe(H_2hcqs}-O,N,O)_n^{(3-2n)+} + 2n\mathrm{H^+}$$

$$K_{\mathrm{eq}} = [\mathrm{Fe(H_2hcqs}-O,N,O)_n^{(3-2n)+}][\mathrm{H^+}]^{2n}/[\mathrm{Fe^{3+}}][\mathrm{H_4hcqs}]^n \quad (1)$$

$$C_{\mathrm{M}} = [\mathrm{Fe^{3+}}] + [\mathrm{Fe(OH)^{2+}}] + [\mathrm{Fe(H_2hcqs}-O,N,O)_n^{(3-2n)+}] \quad (2)$$

$$C_{\mathrm{L}} = [\mathrm{H_4hcqs}] + [\mathrm{H_3hcqs^-}] + n[\mathrm{Fe(H_2hcqs}-O,N,O)_n^{(3-2n)+}] \quad (3)$$

by taking the protonation constants of **1**[2] (*vide infra*) and the hydrolysis constant of iron(III)[3] (*vide infra*) into consideration and by assuming the ligand/metal molar ratio of *n* for the iron(III) complex of **1**. The equilibrium constant, K_{eq}, can be modified into eq. (4) under the experimental conditions of $C_{\mathrm{L}} > 5C_{\mathrm{M}}$ with the use of the total concentration of iron(III), C_{M}, and that of **1**, C_{L}, and of X ($= [\mathrm{Fe(H_2hcqs\text{-}}O,N,O)_n^{(3-2n)+}]/C_{\mathrm{M}}$),

$$K_{\mathrm{eq}} = \{X[\mathrm{H^+}]^{2n}\}/\{(C_{\mathrm{L}} - nXC_{\mathrm{M}})^n(1-X)(1+K_{\mathrm{OH}}/[\mathrm{H^+}])^{-1}\} \quad (4)$$

where K_{OH} is the hydrolysis constant of iron(III) ($\log K_{\mathrm{OH}} = -2.73$ mol dm^{-3} (0.15 mol dm^{-3} $\mathrm{NaClO_4}$), 20°C; $K_{\mathrm{OH}} = [\mathrm{Fe(OH)^{2+}}][\mathrm{H^+}]/[\mathrm{Fe^{3+}}]$).[4] At the isosbestic point of the absorption curves of these two ligand species (502 nm), the parameter X can be related to the absorbance, A_{i}, of a solution in which the complex and ligand species coexist at the acidity of $[\mathrm{H^+}]$ by eq. (5),

$$A_{\mathrm{i}} = A_{\mathrm{max}} - (A_{\mathrm{max}} - A_{\mathrm{min}})X \quad (5)$$

where A_{max} and A_{min} are the absorbances of solutions in which the iron(III) complex does not form at all and does form quantitatively, respectively. From eqs (4) and (5), eq. (6) can be derived.

$$(1+K_{\mathrm{OH}}/[\mathrm{H^+}])[H^+]^{2n} = K_{\mathrm{eq}}\{(A_{\mathrm{i}} - A_{\mathrm{min}})/(A_{\mathrm{max}} - A_{\mathrm{i}})\}\{C_{\mathrm{L}} - nC_{\mathrm{M}}(A_{\mathrm{max}} - A_{\mathrm{i}})/(A_{\mathrm{max}} - A_{\mathrm{min}})\}^n. \quad (6)$$

Experimental data plotted on the relation between A_{i} and $-\log [\mathrm{H^+}]$ in Fig. 2 were simulated with eq. (6) to give a best-fit (cf. solid line 1 in Fig. 2) only with the values of $n = 1$ and $K_{\mathrm{eq}} = 5.00 \times 10$ mol dm^{-3} for the iron(III)–**1** system.

Likewise, a best-fit could only be obtained with $n = 1$ and $K_{\mathrm{eq}} = 6.00 \times 10$ mol dm^{-3} for the iron(III)–**2** system (cf. solid line 2 in Fig. 2). These results indicate that only mono(ligand)iron(III) complex forms in the iron(III)–**1** as well as iron(III)–**2** system.

From the relation,[2]

$$K_{\mathrm{eq}} = \beta_{11}/K_{\mathrm{a(phOH)}}K_{\mathrm{a(qy(or\ na)OH)}} \quad (7)$$

$$\beta_{11} = [\mathrm{Fe(H_2hcqs\text{-}}O,N,O)^+]/[\mathrm{Fe^{3+}}][\mathrm{H_2hcqs^{2-}}] \quad \text{(for ligand 1)}$$

$$= [\mathrm{Fe(Hhcns)}]/[\mathrm{Fe^{3+}}][\mathrm{Hhcns^{3-}}] \quad \text{(for ligand 2)} \quad (8)$$

where $K_{\mathrm{a(phOH)}}$ denotes the protonation constant of the phenolate oxygen (ligands **1** and **2**) and $K_{\mathrm{a(qy(or\ na)OH)}}$ that of the quinolinolate (ligand **1**) or naphtholate (ligand **2**) oxygen, respectively,[2] the stability constant, β_{11}, was calculated to be $\log \beta_{11}$ (mol^{-1} dm^3) $= 18.32 \pm 0.11$ for $\mathrm{Fe(H_2hcqs\text{-}}O,N,O)^+$ and 19.35 ± 0.11 for Fe(Hhcns).

Incidentally, no absorbance change due to the complex formation was noticed for the iron(III)–**3** and –**4** systems under the same experimental conditions.

Comparison of these stability constants with the constant of $\mathrm{Fe(hqs)^+}$ [$\log \beta_{11}$ (mol^{-1} dm^3) = 11.6 (0.1 mol dm^{-3}, 25°C)[5]] allows us to conclude that this kinetic isomerism is based on a thermodynamic origin of a greater stability for the *O-N-O* than for the *N-O* coordination mode in the iron(III)–**1** system.

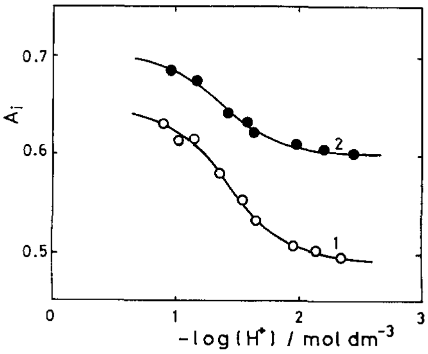

Fig. 2. Dependence of absorbance on $-\log [\mathrm{H^+}]$. 1: C_{L} (ligand **1**) $= 3.62 \times 10^{-5}$ mol dm^{-3}; $C_{\mathrm{M}} = 7.17 \times 10^{-6}$ mol dm^{-3}; wavelength: 502 nm. 2: C_{L} (ligand **2**) $= 3.44 \times 10^{-5}$ mol dm^{-3}; $C_{\mathrm{M}} = 6.78 \times 10^{-6}$ mol dm^{-3}; wavelength: 540 nm; 0.10 mol dm^{-3} ($\mathrm{NaClO_4}$), 22°C.

Kinetics and mechanism

A biphasic kinetic process was observed for the iron(III)–**1** system (cf. Fig. 3), whereas a monophasic process was found on the iron(III)–**2** as well as –**3** and –**4** systems. The faster step of the iron(III)–**1** system and each single step of the other three systems showed the first-order dependence of C_M and of C_L; the slower step of the iron(III)–**1** system, however, was independent of C_M. Accordingly, it is inferred that the faster step is the rate-determining coordination of the first ligand to iron(III) to form a complex with the bidentate *O-N* coordination mode and the slower one is an intramolecular transformation to the terdentate *O-N-O* coordination mode, i.e. a linkage isomerization that has also been found in the aluminium(III) complex of **1**.[2]

$$\mathrm{Fe(OH)}_{3-i}^{i+} + \mathrm{H}_{4-j}\mathrm{hcqs}^{j-} \xrightarrow[\text{fast}]{k_{\mathrm{obs(1)}}}$$

$$\mathrm{Fe(H_2hcqs}-O,N)^+ \xrightarrow[\text{slow}]{k_{\mathrm{obs(2)}}} \mathrm{Fe(H_2hcqs}\text{-}O,N,O)^+$$

The rate equation for the first step can be derived under the conditions of $C_M \gg C_L$ and pH 1.2–2.3, according in principle to a general procedure,[1–3] as follows,

$$\begin{aligned} &\mathrm{d[Fe(H_2hcqs}-O,N)^+]/\mathrm{d}t \\ &\quad = k_{\mathrm{obs(1)}}([\mathrm{Fe(H_2hcqs}-O,N)^+]_{\mathrm{eq}} \\ &\qquad -[\mathrm{Fe(H_2hcqs}-O,N)^+]_t) \qquad (9) \end{aligned}$$

$$\begin{aligned} &k_{\mathrm{obs(1)}}K_{\mathrm{a(qyNH)}}(K_{\mathrm{a(qyOH)}}[\mathrm{H}^+]^2 + K_{\mathrm{a(qyOH)}}[\mathrm{H}^+]+1) \\ &\quad (1+K_{\mathrm{OH}}/[\mathrm{H}^+])/C_M \equiv k_{\mathrm{obs(1)'}} \end{aligned}$$

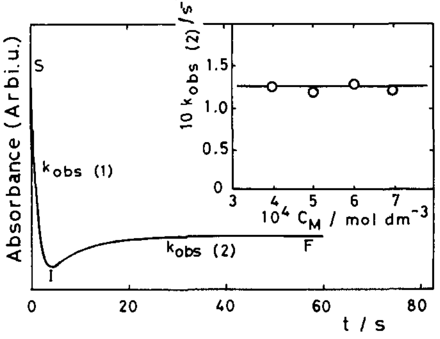

Fig. 3. Absorbance–time course of iron(III)–**1** system. $C_M = 5.00\times10^{-4}$ mol dm^{-3}; $C_L = 3.57\times10^{-5}$ mol dm^{-3}. pH 2.30; wavelength, 502 nm; 0.10 mol dm^{-3} (NaClO$_4$), 22°C. The inset represents relation between $k_{\mathrm{obs(2)}}$ and C_M. Experimental conditions other than C_M are the same as those given above.

$$\begin{aligned} k_{\mathrm{obs(1)'}} &= k_{30}K_{\mathrm{a(qyNH)}}K_{\mathrm{a(qyOH)}}[\mathrm{H}^+]^2 \\ &\quad + (k_{32}+k_{20}K_{\mathrm{a(qyNH)}}K_{\mathrm{OH}})K_{\mathrm{a(qyOH)}}[\mathrm{H}^+] \\ &\quad + k_{33}+k_{22}K_{\mathrm{a(qyOH)}}K_{\mathrm{OH}}+k_{23}K_{\mathrm{OH}}/[\mathrm{H}^+] \qquad (10) \end{aligned}$$

where k_{ij} refers to the formation rate constant of the pathway of $\mathrm{Fe(OH)}_{3-i}^{i+}$ ($i = 2$ and 3) with $\mathrm{H}_{4-j}\mathrm{hcqs}^{j-}$ ($j = 0$, 2 and 3) and ($[\mathrm{Fe(H_2hcqs}\text{-}O,N)^+]_{\mathrm{eq}} - [\mathrm{Fe(H_2hcqs}\text{-}O,N)^+]_t$) corresponds to a net absorbance change of the complex with the bidentate *O-N* coordination mode at time *t*. Additionally, $K_{\mathrm{a(qyNH)}}$ denotes the protonation constant of the quinolyl nitrogen of **1**[2] and $K_{\mathrm{a(qyOH)}}$ has been defined earlier (*vide supra*). Here, assumptions were made that the protonation and deprotonation processes are much faster than the coordination process.[6] Experimental $k_{\mathrm{obs(1)'}}$ vs [H$^+$] data were plotted in the form of the left-hand side of eq. (10) as a function of [H$^+$], which is depicted in Fig. 4(a). A linear relation with the zero intercept gives the best-fit to the experimental data plottings, indicating that the first step proceeds through the parallel pathways of k_{32} and k_{20}.

In the same way, the rate constants were determined for the other iron(III) complex formation systems using the following rate equations.

For the iron(III)–**2** system to form Fe(Hhcns):

$$\begin{aligned} &k_{\mathrm{obs}}(K_{\mathrm{a(naOH)}}K_{\mathrm{a(phOH)}}[\mathrm{H}^+]^2 + K_{\mathrm{a(phOH)}}[\mathrm{H}^+]+1) \\ &\quad \times(1+K_{\mathrm{OH}}/[\mathrm{H}^+])/C_M \equiv k_{\mathrm{obs'}} \\ &k_{\mathrm{obs'}} = k_{31}K_{\mathrm{a(naOH)}}K_{\mathrm{a(phOH)}}[\mathrm{H}^+]^2 \\ &\quad + (k_{32}+k_{21}K_{\mathrm{a(naOH)}}K_{\mathrm{OH}})K_{\mathrm{a(phOH)}}[\mathrm{H}^+] \\ &\quad + k_{33}+k_{22}K_{\mathrm{a(phOH)}}K_{\mathrm{OH}}+k_{23}K_{\mathrm{OH}}/[\mathrm{H}^+]. \qquad (11) \end{aligned}$$

Here, $K_{\mathrm{a(naOH)}}$ and $K_{\mathrm{a(phOH)}}$ are the protonation constants of **2**[2] defined earlier (*vide supra*).

For the iron(III)–**3** system to form Fe(Hcqs)$^+$:

$$\begin{aligned} &k_{\mathrm{obs}}(K_{\mathrm{a(qyNH)}}K_{\mathrm{a(qyOH)}}[\mathrm{H}^+]^2 + K_{\mathrm{a(qyOH)}}[\mathrm{H}^+]+1) \\ &\quad \times(1+K_{\mathrm{OH}}/[\mathrm{H}^+])/C_M \equiv k_{\mathrm{obs'}} \\ &k_{\mathrm{obs'}} = k_{30}K_{\mathrm{a(qyNH)}}K_{\mathrm{a(qyOH)}}[\mathrm{H}^+]^2 \\ &\quad + (k_{32}+k_{21}K_{\mathrm{a(qyNH)}}K_{\mathrm{OH}})K_{\mathrm{a(qyOH)}}[\mathrm{H}^+] \\ &\quad + k_{33}+k_{22}K_{\mathrm{a(qyOH)}}K_{\mathrm{OH}}+k_{23}K_{\mathrm{OH}}/[\mathrm{H}^+]. \qquad (12) \end{aligned}$$

Here, $K_{\mathrm{a(qyNH)}}$ and $K_{\mathrm{a(qyOH)}}$ are the protonation constants of the quinolyl nitrogen and quinolinolate oxygen of **3**,[2] respectively.

For the iron(III)–**4** system to form Fe(hqs)$^+$:

$$\begin{aligned} &k_{\mathrm{obs}}(K_{\mathrm{a(qhNH)}}K_{\mathrm{a(qyOH)}}[\mathrm{H}^+]^2 + K_{\mathrm{a(qyOH)}}[\mathrm{H}^+]+1) \\ &\quad \times(1+K_{\mathrm{OH}}/[\mathrm{H}^+])/C_M \equiv k_{\mathrm{obs'}} \end{aligned}$$

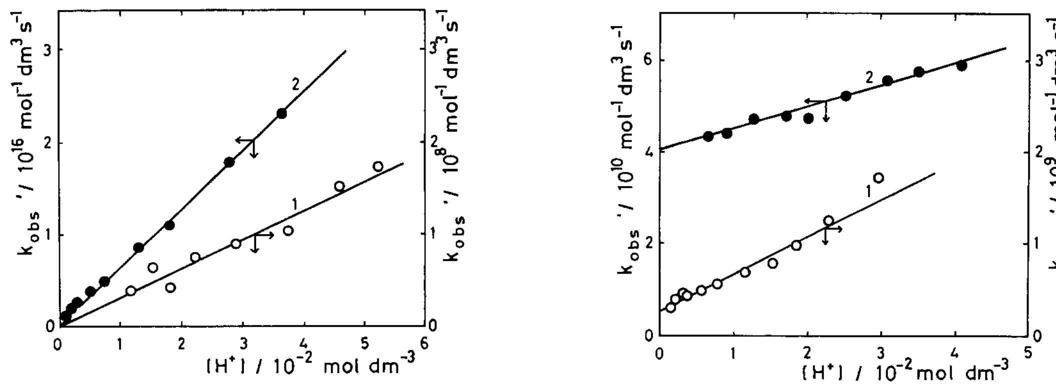

Fig. 4. Relation between $k_{obs'}$ and [H$^+$] for iron(III)-**1**, -**2**, -**3** and -**4** systems; 0.10 mol dm^{-3} (NaClO$_4$), 22°C. (a) Iron(III)-**1** (line 1) and -**2** (line 2) systems. 1 : $k_{obs'} \equiv k_{obs(1)'}$; $C_M = 5.00 \times 10^{-4}$ mol dm^{-3}; $C_L = 3.57 \times 10^{-5}$ mol dm^{-3} (ligand **1**); wavelength, 502 nm; 2 : $C_M = 4.98 \times 10^{-4}$ mol dm^{-3}; $C_L = 3.44 \times 10^{-3}$ (ligand **2**); wavelength, 540 nm. (b) Iron(III)-**3** (line 1) and -**4** (line 2) systems. 1 : $C_M = 5.00 \times 10^{-4}$ mol dm^{-3}; $C_L = 3.47 \times 10^{-5}$ mol dm^{-3} (ligand **3**); wavelength, 497 nm. 2 : $C_M = 5.04 \times 10^{-4}$ mol dm^{-3}; $C_L = 5.03 \times 10^{-5}$ mol dm^{-3} (ligand **4**); wavelength, 605 nm.

$$k_{obs'} = k_{30}K_{a(qyNH)}K_{a(qyOH)}[H^+]^2 + (k_{31}+k_{20}K_{a(qyNH)}K_{OH})K_{a(qyOH)}[H^+] + k_{32}+k_{21}K_{a(qyOH)}K_{OH}+k_{22}K_{OH}/[H^+]\}. \quad (13)$$

Here, $K_{a(qyNH)}$ and $K_{a(qyOH)}$ are the protonation constants of the quinolyl nitrogen and quinolinolate oxygen of **4**,[7] respectively.

Experimental $k_{obs'}$ vs [H$^+$] data were also plotted in the same forms as that of the iron(III)-**1** system, which are depicted in Figs 4(a) [iron(III)-**2** system] and (b) [iron(III)-**3** and -**4** systems]. Linear relations with the zero intercept for the iron(III)-**2** system and non-zero intercepts for the other two systems give the best-fit to the data plottings. The reaction pathways and corresponding rate constants thus estimated are compiled in Table 1.

It is evident from Table 1 that there exists a proton ambiguity in the reaction kinetics of iron(III) with **1**. Therefore, it is natural to start this coordination-kinetic discussion based on the composite rate constants. A comparison of the composite rate constant of the iron(III)-**1** system, $k_{32}+k_{20}K_{a(qyNH)}K_{OH}$, with those constants of the iron(III)-**2**, -**3** and -**4** systems as a first approximation implies that the constant of the iron(III)-**1** system is of the same magnitude as the constants of the iron(III)-**3** ($k_{32}+k_{21}K_{a(qyNH)}K_{OH}$) and -**4** ($k_{31}+k_{20}K_{a(qyNH)}K_{OH}$) systems but is rather smaller than the constant of the iron(III)-**2** system ($k_{32}+k_{21}K_{a(naOH)}K_{OH}$), suggesting that the mechanistic reaction characteristic may be slightly different for the iron(III)-**1**, -**3** and -**4** systems and

Table 1. Kinetic parameters

Ligand	Pathway	k_{ij} (mol^{-1} dm^3 s^{-1})
1	$Fe^{3+} + H_2hcqs^{2-}(k_{32})$	$k_{32}+k_{20}K_{a(qyNH)}K_{OH}$: $(1.92 \pm 0.35) \times 10^3$
	and $FeOH^{2+} + H_4hcqs(k_{20})$	(k_{20} : $(1.06 \pm 0.40) \times 10^3$)^a
2	$Fe^{3+} + H_2hcns^{2-}(k_{32})$	$k_{32}+k_{21}K_{a(naOH)}K_{OH}$: $(8.54 \pm 0.25) \times 10^6$
	and $FeOH^{2+} + H_3hcns^{-}(k_{21})$	(k_{21} : $(8.15 \pm 0.30) \times 10^2$)^a
3	$Fe^{3+} + Hcqs^{2-}(k_{32})$	$k_{32}+k_{21}K_{a(qyNH)}K_{OH}$: $(9.29 \pm 0.34) \times 10^2$
	and $FeOH^{2+} + H_2cqs^{-}(k_{21})$	(k_{21} : $(1.81 \pm 0.40) \times 10^3$)^a
	$Fe^{3+} + cqs^{3-}(k_{33})$	$k_{33}+k_{22}K_{a(qyOH)}K_{OH}$: $(3.83 \pm 0.30) \times 10^8$
	and $FeOH^{2+} + Hcqs^{2-}(k_{22})$	(k_{22} : $(8.00 \pm 0.34) \times 10^3$)^a
4	$Fe^{3+} + Hhqs^{-}(k_{31})$	$k_{31}+k_{20}K_{a(qyNH)}K_{OH}$: $(6.17 \pm 0.25) \times 10^2$
	and $FeOH^{2+} + H_2hqs(k_{20})$	(k_{20} : $(2.75 \pm 0.30) \times 10$)^a
	$Fe^{3+} + hqs^{2-}(k_{32})$	$k_{32}+k_{21}K_{a(qyOH)}K_{OH}$: $(3.44 \pm 0.21) \times 10^{10}$
	and $FeOH^{2+} + Hhqs^{-}(k_{21})$	(k_{21} : $(1.79 \pm 0.26) \times 10^4$)^a

At 0.10 mol dm^{-3} (NaClO$_4$), 22°C.

[a] The values of k_{2j} (j = 0–2) were tentatively estimated from their composite rate constants under the assumption of the pathway of k_{2j} being predominant.

for the iron(III)–**2** system. Accordingly, discussion will be initiated from the simple systems of the iron(III)–**3** and –**4** ones that have only one coordination mode.

The rate constant of k_{21} for the iron(III)–**4** system and that of k_{22} for the iron(III)–**3** system (cf. Table 1) are of the same magnitude as that for the iron(III)–mug^{2-} complex formation system ($Fe(OH)^{2+} + H_2mug$; k (mol^{-1} dm^3 s^{-1}) = $1.14 \pm 0.30 \times 10^3$)[8] that has been concluded to proceed by the mechanistic rate-determining donation of the phenolato oxygen to the central metal atom. On the basis of these kinetic results and the evidence for a higher affinity to iron(III) of the phenolato oxygen {log β_{11} (mol^{-1} dm^3) = 7.76 [25°C, 0.1 mol dm^{-3} ($NaClO_4$)][9] for the mono (phenolato)iron(III) complex} than of the pyridyl nitrogen (no stability constant data for iron(III) have been reported yet on the pyridine and related heterocyclic ligands), it is reasonable to conclude that the mechanistic rate-determining steps of the formation of the iron(III)–**3** and –**4** complexes, and the iron(III)–**1** complex as well, are the coordination of the phenolato oxygen on the quinoline ring to iron(III). The analogous mechanism with the slow donation of the quinolinolato oxygen to iron(III) might be valid for the iron(III)–**2** complex, however, the chelate ring closure as the mechanistic rate-determining step as in the case of the aluminium(III)–**1** system[2] may be more plausible because k_{21} for the iron(III)–**2** system is somewhat smaller than k_{21} of the iron(III)–**3** and k_{20} of the iron(III)–**1** systems that have equally the same seven-substituted ligand geometrical structure.

Additionally, the composite rate constants for the iron(III)–**1**, –**3** and –**4** systems, all having the *N-O* coordination mode, show the decreasing tendency of $1.92 \pm 0.35 \times 10^3$; $9.29 \pm 0.34 \times 10^2$; and $6.17 \pm 0.25 \times 10^2$ (in mol^{-1} dm^3 s^{-1}), which are in line with the increasing tendency of the protonation constant of the quinolinolate oxygen, log $K_{a(qyOH)}$, of 6.36, 7.40 and 8.42.[2,5] The same tendency has also been found in the complex formation reaction kinetics of these ligands with iron(II),[1] where the mechanistic rate-determining step has been deduced to be the donation of the quinolinolato oxygen to the metal ion. These results substantiate the conclusion deduced above that the rate-determining step of the iron(III)–**1**, –**3** and –**4** systems corresponds to the coordination of the quinolinolato oxygen to iron(III). This conclusion is in line with that drawn in the aluminium(III)–**1** system.[2]

A tentative estimation of each rate constant from the composite one by assuming the predominance of either of them afforded us to give k_{32} (mol^{-1} dm^3 s^{-1}) of $1.92 \pm 0.35 \times 10^3$ and k_{20} (mol^{-1} dm^3 s^{-1}) of $1.06 \pm 0.40 \times 10^3$ for the iron(III)–**1** system. The value of k_{32} is about two orders of magnitude larger than the rate constant of the coordination of phenol(Hphe) to Fe^{3+} ($k = 2.5 \times 10$ mol^{-1} dm^3 s^{-1} for $Fe^{3+} + Hphe$)[10] and of salicylaldehyde (Hsalal) to Fe^{3+} ($k = 2.46 \times 10$ mol^{-1} dm^3 s^{-1} for $Fe^{3+} +$ Hsalal),[11] whereas the value of k_{20} is quite reasonable for the coordination of **1** to $Fe(OH)^{2+}$.[12] Hence, it is natural to infer that the formation of the iron(III) complex of **1** proceeds mainly through the pathway related to the constant k_{20}. The same deduction may be valid for the iron(III)–**2** (predominance of the k_{21} pathway), –**3** (that of the k_{21} and k_{22} pathways) and –**4** (that of the k_{20} and k_{21} pathways) systems, although the contribution of the pathways related to k_{32} and k_{31} cannot be excluded in the iron(III)–**3** and –**4** systems when we compare the magnitudes of these individual values tentatively estimated from the composite rate constants with each other.

The second step of the iron(III)–**1** system corresponds to the linkage isomerization from $Fe(H_2hcqs\text{-}O,N)^+$ to $Fe(H_2hcqs\text{-}O,N,O)^+$. The rate equation can be given as follows:

$$
\begin{aligned}
-\mathrm{d}[Fe(H_2hcqs-N,O)^+]/\mathrm{d}t &= k_{obs(2)}[Fe(H_2hcqs-N,O)^+] \\
k_{obs(2)} &= k_{isom}. \qquad (14)
\end{aligned}
$$

The rate constant, k_{isom}, was calculated from the data depicted in Fig. 3 to be $k_{isom} = 1.3 \pm 0.1 \times 10^{-1}$ s^{-1}.

In conclusion, the iron(III)–**1** system having a high-spin d^5-electronic configuration of the central metal atom shows a linkage isomerism from the *N-O* bidentate to the *O-N-O* terdentate moiety, just as in the aluminium(III)–**1** case having a d^0-electronic configuration, and in contrast to the iron(II)–**1** system which has possibly a high-spin d^6-electronic configuration that shows the selective coordination with the *O-N-O* terdentate moiety.

REFERENCES

1. Z.-P. Bai, H. Einaga and J. Hidaka, *Bull. Chem. Soc. Japan* 1990, **63**, 929.
2. Z.-P. Bai, H. Einaga and J. Hidaka, *Bull. Chem. Soc. Japan* 1988, **61**, 1959.
3. H. Kuno, K. Okamoto, J. Hidaka and H. Einaga, *Bull. Chem. Soc. Japan* 1989, **62**, 2824.
4. C. F. Baes, jr. and R. E. Mesmer, *The Hydrolysis of Cations*, p. 229. Wiley, New York (1976).
5. R. M. Smith and A. E. Martell, *Critical Stability*

Constants, Vol. 2, p. 227. Plenum, New York (1975).

6. M. Eigen, *Pure Appl. Chem.* 1963, **6**, 97.
7. K. Hayashi, T. Ohsawa, K. Okamoto, J. Hidaka and H. Einaga, *J. Coord. Chem.* 1983, **12**, 243.
8. H. Yoshida, T. Ozawa, K. Jitsukawa and H. Einaga, *Polyhedron* 1993, **12**, 1319.
9. D. D. Perrin, *Stability Constants of Metal-Ion Complexes*, Part B, IUPAC Chemical Data Series No. 22, p. 344. Pergamon, Oxford (1979).
10. S. Gouder and J. Stuehr, *Inorg. Chem.* 1974, **13**, 379.
11. P. G. T. Fog and R. J. Hall, *J. Chem. Soc. A* 1971, 1365.
12. Reference 7 and refs cited therein.